Assessment of Nahar biodiesel with TiO$_2$ nanoparticles at increased fuel injection pressure of a diesel engine: Exergy, energy, statistical analysis

Akshay Jain [a,*], Bhaskor Jyoti Bora [a,b,c], Rakesh Kumar [c], Debabrata Barik [d], Nithin Kumar [e,**], Prabhu Paramasivam [f], Raman Kumar [g,h,***], Jasgurpreet Singh Chohan [i], Hasan Sh Majdi [j], Majed Alsubih [k], Saiful Islam [k], Chander Prakash [l], Rahul Kumar [m]

[a] Energy Institute Bengaluru, A Centre of Rajiv Gandhi Institute of Petroleum Technology, Bengaluru, Karnataka, 562157, India
[b] Assam Energy Institute, A Centre of Rajiv Gandhi Institute of Petroleum Technology, Sivasagar, Assam, 785697, India
[c] Rajiv Gandhi Institute of Petroleum Technology, Jais, Amethi, U.P., 229305, India
[d] Department of Mechanical Engineering, Karpagam Academy of Higher Education, Coimbatore, 641021, India
[e] Nitte (Deemed to be University), NMAM Institute of Technology (NMAMIT), Department of Mechanical Engineering, Nitte, 574110, India
[f] Centre for Research Impact & Outcome, Chitkara University Institute of Engineering and Technology, Chitkara University, Rajpura, 140401, Punjab, India
[g] Department of Mechanical and Production Engineering, Guru Nanak Dev Engineering College, Ludhiana, Punjab, 141101, India
[h] Jadara Research Center, Jadara University, Irbid, 21110, Jordan
[i] University Centre for Research & Development, Department of Mechanical Engineering, Chandigarh University, Gharuan, Punjab, India
[j] Department of Chemical Engineering and Petroleum Industries, Al-Mustaqbal University College, Babylon, 51001, Iraq
[k] Civil Engineering Department, College of Engineering, King Khalid University, Abha, 61421, Saudi Arabia
[l] Research and Innovation Cell, Rayat Bahra University, Mohali, 140301, Punjab, India
[m] Department of Mechanical Engineering, Graphic Era (Deemed to be University), Dehradun, 248002, India

ARTICLE INFO

ABSTRACT

There is a need for sustainable diesel alternatives addressing fuel depletion, price instability, and environmental impact. A nanofuel is developed by blending Nahar Biodiesel with a concentration of 150 ppm of TiO$_2$ nanoparticles. The nanofuel, named NBD-TNP, is tested for increased fuel injection pressure (FIP) and variable engine loads (EL). The prepared nanofuel is tested in a 3.5 kW diesel engine. Five FIPs (200–280 bar with 20 bar increments after each set of experiments) and five ELs (20–100 % with 20 % increment after each set of experiments) are used to display the results. NBD-TNP nanofuel showed positive outcomes with an increased FIP of 260 bar. The maximum exergetic efficiency of 40.11 %, the maximum value of BTE of 29.22 %, and the maximum NHRR is 67.86 J/°CA for the FIP of 260 bar for NBD-TNP nano fuel at 100 % engine

* Corresponding author.
** Corresponding author.
*** Corresponding author. Department of Mechanical and Production Engineering, Guru Nanak Dev Engineering College, Ludhiana, Punjab, 141101, India.
E-mail addresses: ajainmech@gmail.com (A. Jain), bhaskorb3@gmail.com (B.J. Bora), rkumar@rgipt.ac.in (R. Kumar), debabrata93@gmail.com (D. Barik), nithinmech33@nitte.edu.in (N. Kumar), lptprabhu@gmail.com (P. Paramasivam), sehgal91@yahoo.co.in (R. Kumar), jasgurpreet.e6524@cumail.in (J.S. Chohan), mn13022020@gmail.com (H.S. Majdi), malsubih@kku.edu.sa (M. Alsubih), sfakrul@kku.edu.sa (S. Islam), chander.mechengg@gmail.com (C. Prakash), rahulkumarmech84@gmail.com (R. Kumar).

load. The lowest CO and HC emission for the NBD-TNP nanofuel at FIP is 260 bar for all ELs. The statistically optimized value obtained from RSM analysis is 47.95 % of EL and 263.45 bar of FIP for optimum values of response variables. The study concludes that the NBD-TNP nanofuel is a promising alternative for diesel fuel at an FIP of 260 bar.

Nomenclature and Abbreviations

BTE	Brake Thermal Efficiency	^{0} bTDC	Degree Before Top Dead Center
BP	Brake Power	^{0}CA	Degree Crank Angle
CV	Calorific Value	A_{in}	Exergy of Fuel
CO	Carbon Monoxide	A_s	Shaft Exergy
CI	Compression Ignition	A_c	Cooling Water Exergy
CO_2	Carbon Dioxide	A_e	Exhaust Gas Exergy
DOE	Design of Experiments	A_d	Exergy Destruction
EGR	Exhaust Gas Recirculation	Q_{in}	Energy of Fuel
EL	Engine Load	Q_s	Shaft Energy
FAME	Fatty Acid Methyl Esters	Q_c	Cooling Water Energy
FIP	Fuel Injection Pressure	Q_e	Exhaust Gas Energy
GHG	Global Greenhouse Gas	Q_u	Unaccounted Losses
HC	Hydrocarbons	kW	Kilo Watts
ID	Ignition Delay		
IT	Injection Timing		
NBD	Nahar Biodiesel		
NBD-TNP	NBD +150 ppm of TiO_2 NPs		
NOx	Oxides of Nitrogen		
RSM	Response Surface Methodology		
SEM	Scanning Electron Microscopy		
TiO_2	Titanium Oxide		
XRD	X-ray Diffraction		

1. Introduction

In 2022, fossil fuels were reported for greater than 80 % of the global energy supply. However, using fossil fuels has dangerous environmental consequences, including contributing majorly to greenhouse gas emissions and pollution [1]. Significant reforms are required for the energy sector to address these challenges, including reducing the use of fossil fuels, improving energy efficiency, and, most importantly, increasing the deployment of renewable energy sources. These reforms will be critical in reducing anthropogenic contributions to climate change and mitigating its impacts [2]. Energy security, climate change, and increasing demand for energy are now among the most pressing international challenges. Experts widely acknowledge that renewable energy has arisen as a key to addressing these challenges. However, it is important to note that the shift to renewable energy cannot be viewed in isolation. Fossil fuel prices significantly impact the growth of renewable energy, particularly in terms of investment and return. Therefore, a comprehensive understanding of the interplay between these two sectors is crucial for effective renewable energy development [3]. Incorporating renewable energy sources in a country's energy mix is a sustainable approach that can reduce dependence on traditional fossil fuels, which can ultimately lead to a decrease in greenhouse gas emissions. The Sustainable Development Scenario (SDS) context is a long-term plan that aims to achieve human and global safety by addressing energy utilization, limiting air pollution, and mitigating the effects of climate change. The SDS proposes a transformation of the energy assortment in the direction of a low-carbon economy, which would involve biofuels derived from biomass [4].

Biofuels, derived from natural biomass, offer a renewable alternative to petroleum and support sustainability goals. Evolving from Generation 1 to Generation 4, their production utilizes chemical or enzymatic catalysts to enhance efficiency and reduce pollution. Oxygenated biofuels promote cleaner combustion, helping to mitigate climate change and support rural economies. Globally, biofuels play a vital role in reducing greenhouse gases, with countries like India incorporating them into energy policies to fulfill Paris Agreement commitments.

By promoting the production and usage of biofuels, India aims to achieve its renewable energy targets while reducing its carbon footprint [5]. Biofuel is a sustainable fuel that reduces carbon dioxide (CO_2) emissions by up to 65 % [6]. Biodiesel is a prevalent biofuel that consists of fatty acid methyl esters (FAME) synthesized from the transesterification process of fats and oils [7]. Various categories of feedstocks are utilized for the synthesis of biodiesel. Eatable oils, namely rapeseed, palm, sunflower, soybean, corn, and canola, are major contributors. Non-edible oil feedstocks like Millettia pinnata, Jatropha curcas, Ricinus communis, and Nicotiana tabacum are also used. Animal-derived feedstocks such as tallow, lard, and poultry fat are also utilized. A recent development is using mixed (hybrid) oil for biodiesel synthesis. Waste oil feedstocks from restaurants and food processing plants, such as recycled oil and grease, have been used to minimize environmental issues [8].

Waste plastics oil blend (WPB) was used in place of traditional diesel fuel in a study by Mohan et al. [9] to examine the performance of diesel engines. Using a direct-injection diesel engine with a 17.5 compression ratio and 210 bar fuel injection pressure, they evaluated WPB at 20 %, 40 %, and 100 % mixes. Advanced fuel injection timing (AFIT) was modified from 17.5° to 25.0° in 2.5°

increments, while the engine load varied from 0 % to 100 % in 25 % increments. The findings demonstrated that, in comparison to standard diesel, maximizing AFIT enhanced engine performance and energy conversion from WPB. Rajak et al. [10] examined the effects on engine performance and emissions at constant speeds (2000–3000 rpm) under a full load of adding zinc oxide (ZnO) nanoparticles at concentrations of 0.025 %, 0.05 %, and 0.1 % to diesel fuel. They discovered that the 0.1 % ZnO mix decreased specific fuel consumption by 1.67 %, exhaust gas temperature by 11.4 %, NOx emissions by 10.67 %, and CO2 emissions by 7.6 % while increasing brake thermal efficiency by 11.7 % and cylinder pressure by 2.3 % at 2500 rpm. ZnO nanoparticle additions increased engine efficiency and decreased pollutants, with numerical results matching experimental data. Singh et al. [11] used experimental and numerical techniques to study a fixed-type anaerobic digester (AD) to generate biogas. Over 30 days, the AD was painted black to improve heat absorption, and cow dung was added every six days to stimulate microbial development, raising the digester's temperature by 6–7 °C. The total amount of gas produced was 0.00503 m^3. The numerical study used CFD with tetrahedral meshing and the SIMPLE method. The inoculum's pH stayed between 7.1 and 7.2, which is appropriate for synthetic fertilizer. Tiwari et al. [12] used ANN and RSM to maximize biodiesel production from 30 % cottonseed and 70 % spirulina microalgae oil. They reported NOx emissions rose by 14 % and 18.3 %, respectively. HBD and HBD20's CO2 emissions were 2.49 % and 8.30 % lower than diesel's. At 363 °C, the maximum cylinder pressure recorded was 66.87. Recent studies have explored the transient lubrication dynamics within diesel engine fuel supply mechanisms, highlighting the importance of optimizing cam-roller interactions for enhanced engine efficiency [13]. Understanding the thermal-pressure coupling effect on bearings is essential for improving engine performance, as demonstrated in recent research on journal-thrust coupled bearings [14].

The importance of biodiesel is increasingly recognized in the battle for clean energy and environmental preservation. Biodiesel, produced from sustainable resources like algae, animal fats, and vegetable oils, serves as an alternative to fossil fuels. Its ability to reduce greenhouse gas emissions and dependence on non-renewable energy sources highlights its significance. Biodiesel enhances energy security by decreasing reliance on petroleum and bolstering local economies through job creation. Its closed carbon cycle helps to lower greenhouse gases, and reduced emissions of sulfur oxides, particulate matter, and hydrocarbons improve air quality. Sustainable production methods utilizing microalgae and non-food plants minimize environmental impact and preserve biodiversity. As technology advances, biodiesel's role in creating a cleaner, more resilient energy system continues to expand.

Nahar or Mesua Ferrea, or Ironwood, Indian rose chestnut, and Nagkeshar is a tree species found in India, Southeast Asia, and Sri Lanka [15]. Its seeds are rich in oil content, with up to 65 % of weight. This oil can be used to produce biodiesel. The Konkan, northeast region, Karnataka, Andaman, and Deccan peninsula, in India, have favorable settings for the growth of Nahar plants. Assam, one of the major states in India, produces more than 10 million kg of Nahar seeds annually [16]. Dhawane et al. [17] synthesized biocatalysts of coconut shells and used them to transesterify Nahar seed oil. Bora et al. [18] obtained biodiesel from Nahar seed shell oil. Bora et al. [19] made emulsions from Nahar seed oil and alcohol using 2-butanol as a surfactant to generate hybrid fuel. The properties of produced fuels were similar to biodiesel and diesel. Bordoloi et al. [20] concluded that the pyrolyzed Nahar seed shells and Pongamia Glabra generated bio-oil, and the sub-fractions can be used as renewable fuels. Kushwah et al. [21] observed that blending up to 15 % of the Nahar oil in diesel can be utilized without any modification in a diesel engine. Dash et al. [22] reported that blending 40 % Nahar biodiesel (NBD) with diesel may be utilized in diesel engines. Dash et al. [23] suggested applying NBD blends up to B40 for gensets and agricultural units. Dabi et al. [24] reported that blending 10 % Nahar seed oil gives comparable results to diesel. A distinguished development in brake thermal efficiency (BTE) and reduction in the emissions of carbon monoxide (CO) and oxides of nitrogen (NOx) were reported with the application of 5 % and 10 % diethyl ether with a blend of Nahar oil and diesel. The utilization of ethanol increased BTE. However, brake specific fuel consumption was intensified. NOx, CO, and hydrocarbons (HC) emissions were decreased [25]. Applying 10 % ethyl alcohol with a blend (20 % Nahar oil + 80 % diesel) enhanced BTE and decreased emissions of CO; however, it amplified the emission of NOx [26].

Machine learning techniques have demonstrated promise in predicting propulsion power and resistance in marine systems [27] (Zhou et al., 2023; Sun et al., 2024), indicating potential applications for optimizing diesel engine parameters through statistical methods like RSM [28]. Advanced data fusion techniques have enhanced fault diagnosis in machine systems, offering insights for optimizing diesel engine performance [29]. The adoption of sustainable aviation fuels has shown significant reductions in particulate matter emissions, underscoring the potential of alternative fuels such as NBD-TNP nanofuel in lowering diesel engine emissions [30]. Improved heat transfer and endothermic pyrolysis have been found to enhance combustion performance, mirroring the observed effects of TiO_2 nanoparticles in diesel engines [31].

Biodiesel exhibits higher viscosity and density than diesel, which can lead to atomization issues and negative impacts on the fuel system, including clogging of fuel injectors. To address these concerns, researchers have focused on reducing biodiesel's density and viscosity while optimizing diesel engine operating parameters for improved performance, lower emissions, and better combustion characteristics. Adjusting injection timing (IT) and pressure can yield even better results for diesel engines [32]. The fuel injection pressure (FIP) significantly impacts diesel engines' fuel atomization and mixture preparation. Therefore, it is crucial to identify the optimal FIP for diesel engines [33]. Increasing the FIP can significantly reduce smoke emissions and fuel consumption across all pilot injection modes while maintaining acceptable NO emissions levels. Higher FIP can also reduce soot particles in both accumulation and nucleation modes, which ultimately results in an overall reduction in soot emissions [34]. A study found that increasing FIP enhances fuel atomization and other spray characteristics, improving combustion. This results in higher BTE and lower emissions of HC, CO, and smoke in the engine exhaust compared to diesel. Therefore, using a biodiesel blend in diesel with increased FIP can lead to improved engine characteristics [35].

Nanoparticles (NPs) are being integrated into biodiesels and their blends to enhance fuel characteristics. Adding NPs leads to increased reaction surface area, facilitating better heat transfer between fuel droplets and air. This, in turn, reduces ignition delays and improves the combustion process. Metal NPs are an effective fuel nano-additive, as they possess superior heat transfer characteristics

and higher catalytic activities. This results in complete combustion and enhanced engine performance through increased BTE and decreased fuel consumption. However, incorporating NPs can result in an increment of the in-cylinder temperature, which, in some studies, has been shown to raise the NOx emissions [36]. Incorporating NPs with high thermal conductivity has been found to significantly improve fuel combustion's thermal performance. Specifically, it enhances the thermal characteristics of both the un-burned fuel particles and flame front, accelerating the fuel vaporization rate and preparing a more combustible mixture. This finding has important implications for designing and optimizing combustion systems, particularly those used in high-performance engines and power generation applications [33,37]. NPs can improve the volumetric energy density of liquid fuel, thereby reducing ignition lag by boosting heat transfer rates. When biofuels are infused with nanoparticles, the fuel properties, specifically the heating value, are improved due to the higher surface area-to-volume ratio. The integration of nanoparticles in fuel helps better mix with air, atomization, and vaporization processes. In Nano fuel, TiO_2 NPs act as an oxidation catalyst, allowing more oxygen to reach the fuel flame in the cylinder, which results in better combustion and lower CO emissions. TiO_2 NPs activation energy also burns the carbon particles, thereby decreasing HC emissions [38].

Exergy and energy analysis are powerful tools that engineers use to optimize the performance of engines. By examining the maximum output an engine can produce, engineers can design improved systems and enhance the efficiency of existing ones. Exergy analysis provides a comparative index that combines the first and second laws of thermodynamics to describe the performance of thermal systems. By reducing energy losses, engineers can improve the efficiency of these systems and achieve better results [39]. The analysis of energy consumption in diesel engine combustion processes is the primary focus of the first law of thermodynamics. However, this law does not account for energy quality. Therefore, it is necessary to utilize the second law of thermodynamics, which involves exergy analysis of the diesel engine control volume, to assess the energy quality of the system. The second law is particularly crucial in evaluating energy quality. Exergy analysis is a measure of the work potential of a system, which can be employed to determine its physical and chemical work potential [40].

Non-linear methods such as DoE, artificial neural networks, fuzzy logic, Taguchi methods, genetic algorithms, and RSM are used to analyze multivariate data. RSM, which is derived from DoE, optimizes system performance by evaluating the combined effects of multiple variables. Its primary advantage is that it reduces testing time and costs by developing an optimal test matrix, which facilitates the efficient identification of ideal operational parameters.

Integrating nanoparticles and Nahar Biodiesel into diesel engines offers both possibilities and obstacles to improving fuel economy, cutting emissions, and maximizing engine performance. One of the main concerns is the effect of the viscosity and density of biodiesel on engine atomization, combustion efficiency, and overall fuel system performance. Furthermore, a detailed analysis of the efficacy of adding nanoparticles—particularly TiO_2 nanoparticles—to biodiesel blends is necessary to comprehend how they contribute to improved combustion characteristics, shorter ignition delays, and improved thermal performance. Optimizing engine parameters, such as fuel injection pressure (FIP), timing of injection (IT), and engine load (EL), is also crucial to increase brake thermal efficiency (BTE) and minimize emissions of nitrogen oxides (NOx), hydrocarbons (HC), and carbon monoxide (CO). To evaluate the energy quality of blends of biodiesel and nanoparticles and optimize engine systems for maximum output and efficiency, it is imperative to employ exergy and energy analysis techniques. This will help develop sustainable and effective biofuel solutions that align with international efforts to combat climate change and reduce greenhouse gas emissions.

This study aims to perform the thermodynamic, performance, and emissions analysis on the nanofuel produced from blending Nahar Biodiesel with TiO_2 nanoparticles at varying FIP and EL. In this regard, a single-cylinder water-cooled diesel engine with a provision of varying the FIP and EL is considered. The combination of five FIP values (200–280 bar with 20 bar increment after each set of experiments) and five ELs (20–100 % with 20 % increment after each experiment) are proposed for the test run and lead to the following research objectives.

- Evaluate the performance of Nahar Biodiesel blended with TiO2 nanoparticles (NBD-TNP) in a diesel engine.
- Investigate the effects of increased fuel injection pressure (FIP) on the efficiency and emissions of NBD-TNP nanofuel.
- Analyze the thermodynamic properties, specifically exergetic efficiency and brake thermal efficiency (BTE), of NBD-TNP nano fuel under varying engine loads (ELs).
- Assess the emissions characteristics, including CO and HC emissions, of NBD-TNP nanofuel at different FIPs and ELs.
- Optimize the engine parameters, such as FIP and EL, using statistical analysis (Response Surface Methodology, RSM) to identify the most efficient and environmentally friendly operating conditions for NBD-TNP nanofuel.
- Conclude the study by determining the suitability of NBD-TNP nanofuel as a promising alternative to diesel fuel, particularly at an FIP of 260 bar.

This study is important because it helps solve important issues in the energy and automobile industries. The project intends to give insights into the viability of employing nano fuels as sustainable alternatives to conventional diesel by analyzing Nahar Biodiesel combined with TiO2 nanoparticles (NBD-TNP) in a diesel engine. The study of varied engine loads (ELs) and increasing fuel injection pressure (FIP) provides important information on improving fuel economy and cutting emissions, essential for minimizing environmental effects and adhering to strict regulations. It is easier to understand the dynamics of NBD-TNP nanofuel performance under varied operating situations by analyzing its thermodynamic properties and emissions characteristics. Furthermore, engine characteristics that maximize efficiency and minimize emissions may be found by applying statistical optimization techniques.

2. Material and methods

2.1. Nahar seed oil biodiesel production

The authors have previously provided a detailed analysis of the Nahar biodiesel (NBD) production process [41], as portrayed in Fig. 1 (a). The determination of properties of fuels are based on ASTM-D-6751-20a standards, which are listed in Table 1. The measured density of NBD-TNP is 885.01 kg/m^3, compared to 885 kg/m^3 for the NBD. This extremely small difference of approximately 0.002 % is negligible and does not influence the energy calculation. Since the lower calorific value is expressed on a per-mass basis, such a minor variation in density does not affect the fuel's overall energy content or performance evaluation. To determine the size and crystallographic arrangement of TiO$_2$ nanoparticles, scanning electron microscopy (SEM) and X-ray diffraction (XRD) techniques were employed, aligning with recent advancements in spectroscopic analysis of combustion particles [42]. and the results are shown in Fig. 1 (b) and 1 (c). Biodiesel research has significantly benefited from SEM, which offers in-depth knowledge of the morphology and microstructure and makes it possible to characterize feedstocks, including microalgae and vegetable oils, by exposing their cell structures and surface appearance. Analyzing the catalysts' nanostructure and particle dispersion also contributes significantly to the evaluation of the catalysts and increases catalytic efficiency. By identifying contaminants and examining byproducts like glycerol, SEM helps with quality control by guaranteeing the integrity of the finished biodiesel product. The concentration of NPs is used as 1 ppm = 1 mg/L [43]. Fig. 1 (d) represents the process used for NBD-TNP nanofuel preparation. A concentration of 150 ppm of TiO$_2$ NPs was blended with NBD to generate NBD-TNP nanofuel.

2.2. Specification of research engine

The experiment was conducted using a test engine, stationary type powered with diesel and biodiesel blends that adjusted various operational parameters such as compression ratio, engine load, and FIT, as depicted in Fig. 2(a) and (b). A detailed explanation of the engine can be found in Table 2. An experimental matrix was formulated to design the experiment and is depicted in Fig. 2 (c).

2.3. Emission analysis

The Testo-five flue gas analyzer is a tool used to measure exhaust emissions. It works by attaching a probe to the exhaust manifold to measure the emissions of CO, CO$_2$, HC, and NOx. The values of these emissions are displayed on the gas analyzer's display unit. The accuracy and specification data of the analyzer have already been disclosed previously [44,45].

2.4. Uncertainty analysis

Each experiment in this study was conducted three times. Additionally, an uncertainty analysis was performed to ensure precision and accuracy. Perturbation techniques are a powerful tool for calculating experimental uncertainties associated with complex mathematical models [46]. These techniques are instrumental when the system under study has a complex mathematical model, and the parameters involved in the model are uncertain. Perturbing the model's input parameters helps estimate the impact of the uncertainties on the model's output. This allows for a more precise and accurate characterization of the overall uncertainty associated with experimental results. The visualizations in Fig. 3a and (b) effectively convey the amount of the relative errors and uncertainties
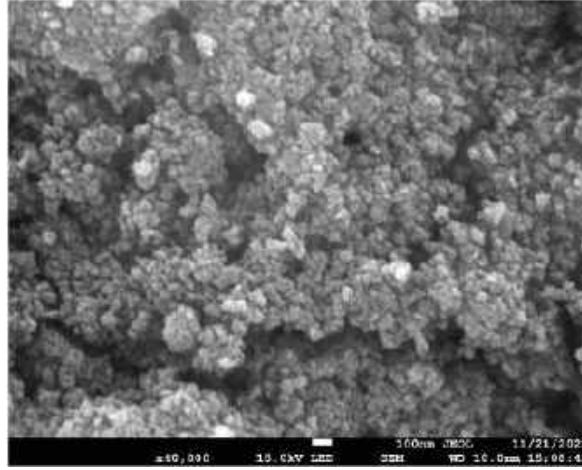

Fig. 1 (a). Steps for Nahar oil production.

Table 1

Test Fuel's characteristic.

Property	NBD	NBD + TNP	Diesel
Lower Calorific Value (MJ/kg)	38.04	40.21	42.3
Density (kg/m^3)	**885**	**885.01**	**842**
Viscosity cSt@40 °C	5.93	–	2.71
Cloud Point (K)	271	–	272
Fire Point (K)	427	430	357
Flash Point (K)	416	420	347
Cetane Number	51.3	55	45

Fig. 1 (b). SEM imaging of TiO$_2$ NPs.

related to several parameters.

2.5. Thermodynamic analysis

Real-time condition monitoring of engine components, such as bearings, is essential for assessing performance and durability [47]. During the expansion stroke, the chemical energy of the fuel is released and represented by Ref. [48]. This energy is further classified into different forms, such as shaft energy (Qs), energy carried by the cooling water (Qw), energy gained by the exhaust gas (Qe), and unaccounted energy losses (Qu). The available energy or exergy of the fuel is represented by Ain, which is also divided into shaft exergy (As), exergy carried by the cooling water (Aw), exergy gained by the exhaust gas (Ae), and exergy destruction (Ad). To carry out energy and exergy analysis, several equations are used that help in measuring the amount of energy and exergy available in various forms as follows:

The delivery rate of fuel energy can be calculated by dividing the total energy by the unit time [44]:

$$Q_{in} = [\dot{m}_{di} \times LHV_{di}], kW \qquad \text{Eq. [1]}$$

The brake power measurement will be determined through a technical process that involves calculating the power output of a braking system. This measurement is crucial in evaluating the performance and efficiency of the braking system [44]:

$$BP = \frac{2 \times \pi \times N \times W \times r}{60 \times 1000}, Kw \qquad \text{Eq. [2]}$$

The BTE calculation involves quantifying the proportion of the energy released by fuel during the combustion process that gets converted into useful work by an engine. This is determined by comparing the engine's network output against the amount of heat energy released by the fuel [44]:

$$BTE = \frac{BP \times 3600 \times 100}{Q_{in}}, \% \qquad \text{Eq. [3]}$$

The term "pressure smoothing" refers to a process that involves the reduction of abrupt pressure changes in a fluid flow. It is achieved by applying mathematical algorithms that smooth out the pressure variations, resulting in a more consistent flow [49]:

$$P_n = \frac{(P_{n-1}) + 2(P_n) + (P_{n+1})}{4} \qquad \text{Eq. [4]}$$
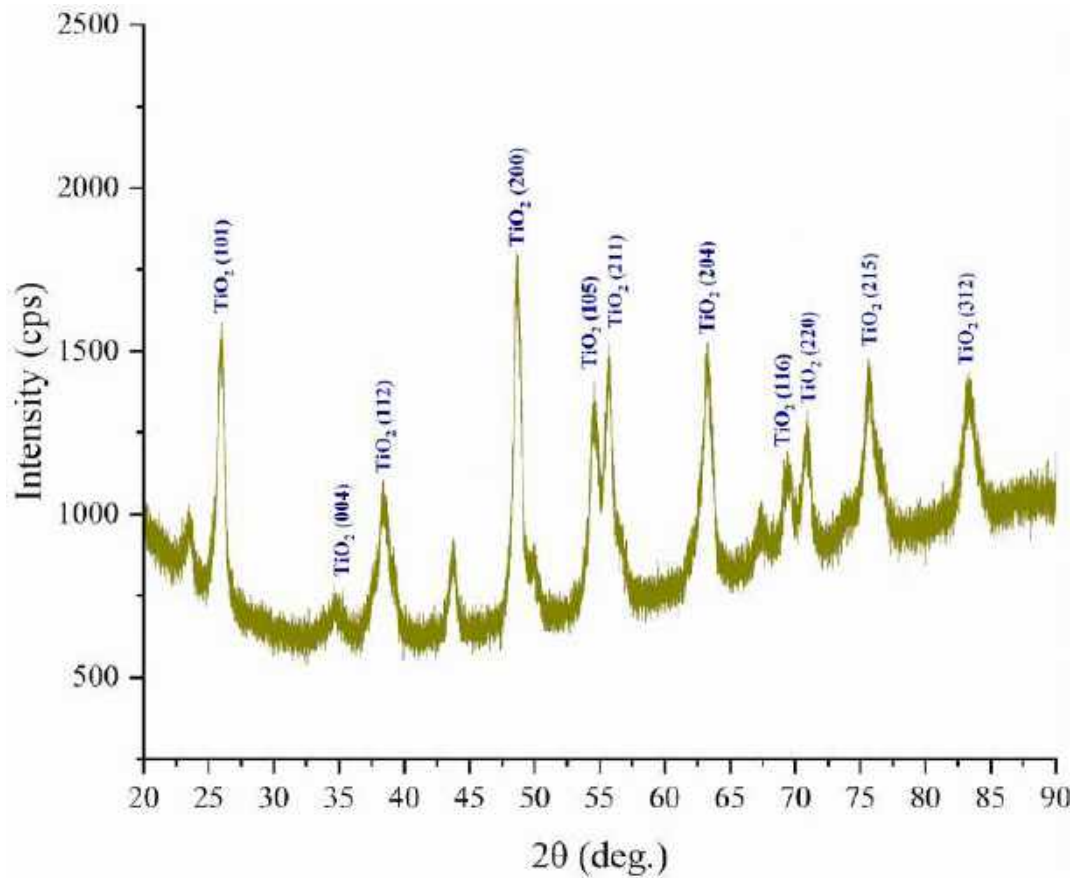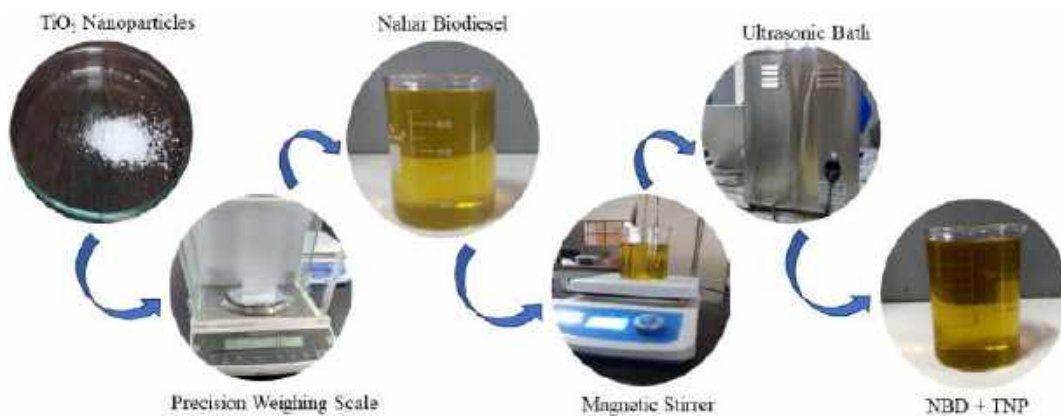
Fig. 1 (c). XRD imaging of TiO₂ NPs.

Fig. 1 (d). Steps for NBD-TNP nanofuel.

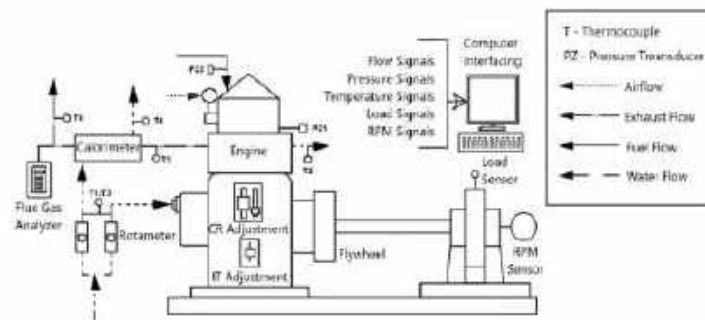The following formula can be used to calculate the rate of pressure rise [44]:

$$\frac{dP}{d\theta} = \frac{(P_{n-2}) - 8(P_{n-1}) + 8(P_{n+1}) - (P_{n+2})}{12(\Delta\theta)}$$

Eq. [5]

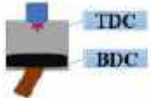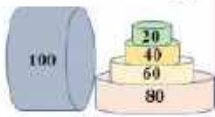Net heat release rate (NHRR) [$\frac{dQ_n}{d\theta}$] can be calculated as [44]:

(a). Engine Pictorial View

(b). Schematic of Engine

Operating Parameter of the Engine		Operating Parameter for Diesel	Operating Parameter for NBD-TNP				
o Compression Ratio	17.5	17.5	17.5				
o Engine Speed [RPM]		1500	1500				
o Injection Timing [deg. bTDC]	TDC BDC	23	23				
o Fuel Injection Pressure [bar]		200	200	220	240	260	280
o Engine Load %	20 40 60 80 100	20% 40% 60% 80% 100%	20% 40% 60% 80% 100%	20% 40% 60% 80% 100%	20% 40% 60% 80% 100%	20% 40% 60% 80% 100%	20% 40% 60% 80% 100%

(c). Experimental Matrix

Fig. 2. Engine setup and experimental matrix.**(a)**. engine pictorial view **(b)**. Schematic of engine **(c)**. Experimental matrix

Table 2
Specifications of engine.

| Parameter	Specifications
Engine Type	Research Engine test setup
No. of Cylinder	1
Injection Timing	23^0bTDC (Range from 0 to 35^0bTDC)
Injection Pressure	200 bar (Range from 200 to 280 bar)
Dynamometer	Eddy current type, 0–12 kg, 185 mm radius
Fuel Injector	3 - Holes having dia. = 0.3 mm, sprays at $120°$ angle of spray
Rated Output	3.5 kW at 1500 rpm
Bore and Stroke	0.087 m $\times$ 0.110 m
Capacity	661 cc
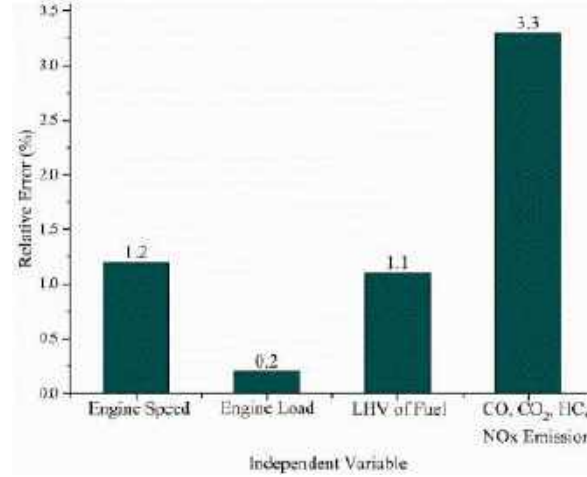
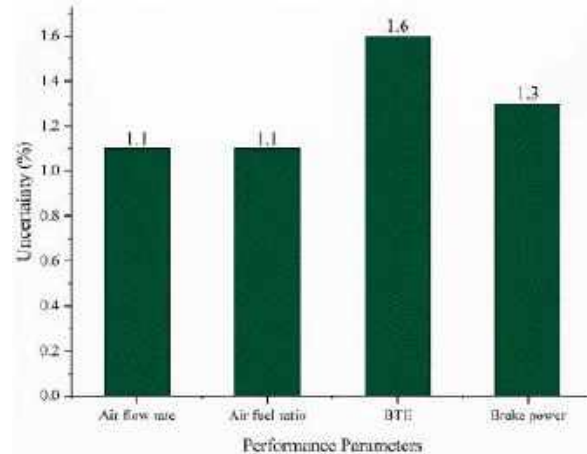**Fig. 3 (a).** Relative error of parameters.

Fig. 3 (b). Uncertainty of various parameters.

$$\frac{dQ_n}{d\theta} = \left(\frac{\gamma}{\gamma - 1} \times P \times \frac{dV}{d\theta} \right) + \left(\frac{1}{\gamma - 1} \times V \times \frac{dP}{d\theta} \right)$$

Eq. [6]

Ignition delay (ID) is a fundamental parameter in combustion science that refers to the time interval between the instant of fuel injection (θ_{IN}) and the crank angle at which the combustion process begins (θ_{IG}) [50]:

$$ID = \theta_{IG} - \theta_{IN}, ° CA$$

Eq. [7]

The process of transferring heat energy from a system to its surroundings can be quantified by measuring the rate at which water

cools down. This rate of heat transfer can be expressed mathematically [44]:

$$Q_C = \left[\dot{m} \times C_{pw} \times (T_{woe} - T_{wie})\right], kW \qquad \text{Eq. [8]}$$

One can calculate the energy dissipation rate through exhaust gas by analyzing its time-dependent behaviour [44]:

$$Q_e = \left[(m_a + \dot{m}_{di}) \times C_{pe} \times (T_{eic} - T_{amb})\right], kW \qquad \text{Eq. [9]}$$

The specific heat value provides essential data for the design and optimization of energy systems and equipment that involve the use of exhaust gases [44]:

$$C_{pe} = \frac{\left[\dot{m}_{wic} \times C_{pw} \times (T_{woc} - T_{wic})\right]}{[(\dot{m}_a + \dot{m}_{di}) \times (T_{eic} - T_{eoc})]}, \frac{kJ}{kgK} \qquad \text{Eq. [10]}$$

The quantification of energy dissipation rate involves calculating the loss of energy per unit time, which cannot be directly measured [49]:

$$Q_u = [Q_{in} - (Q_s + Q_c + Q_e)], kW \qquad \text{Eq. [11]}$$

The availability of a system can be measured and determined using technical methods and tools [44]:

$$A_{in} = \frac{[(1.0338 \times \dot{m}_{di} \times LHV_{di})}{3600}, kW \qquad \text{Eq. [12]}$$

The evaluation of the shaft's accessibility can be carried out [44]:

$$A_s = Brake\ power, kW \qquad \text{Eq. [13]}$$

The expression for determining the availability of cooling water is as follows [44]:

$$A_w = \left[Q_c - \dot{m}_{we} \times C_{pw} \times T_{amb} \times ln\left(\frac{T_{woe}}{T_{wie}}\right)\right], kW \qquad \text{Eq. [14]}$$

An evaluation is underway to determine the availability of exhaust gas emissions [44]:

$$A_e = Q_e + \left[(\dot{m}_a + \dot{m}_{di}) \times T_{amb} \times \left\{C_{pe} \times ln\left(\frac{T_{amb}}{T_{eic}}\right) - R_e \times ln\left(\frac{P_{amb}}{P_e}\right)\right\}\right], kW \qquad \text{Eq. [15]}$$

The formula for calculating the availability destruction can be expressed as [44]:

$$A_d = [A_{in} - (A_s + A_w + A_e)], kW \qquad \text{Eq. [16]}$$

The exergetic efficiency, which is the ratio of the actual work output to the minimum thermodynamic work input required for a
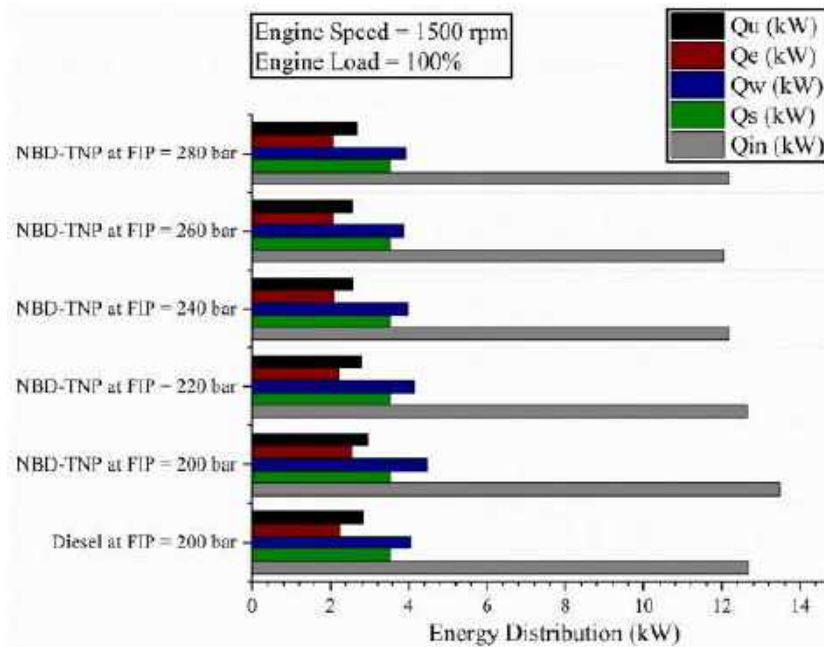

Fig. 4(a). Energy Distribution (kW) for different FIPs at 100 % EL.

process, is a fundamental parameter that determines the level of irreversibility and inefficiency in a thermodynamic system [44]:

$$\eta_{II} = \left[1 - \left(\frac{A_d}{A_{in}} \right) \right] \times 100\% \qquad \text{Eq. [17]}$$

One can assess the production of entropy by a system through a process called entropy generation analysis [51]:

$$S = \frac{A_d}{T_{amb}}, \frac{kW}{K} \qquad \text{Eq. [18]}$$

3. Results and discussion

3.1. Energy and exergy study

The engine receives energy from the fuel's chemical energy and the intake air's energy. This energy is then converted into power output, energy in the exhaust gas, and heat transfer. Analysing energy and exergy usage can offer valuable insights into the sustainability, feasibility, and optimization potential of fuel [42]. This analysis can shed light on the efficiency of energy and exergy, as well as areas where improvements can be made to reduce losses. A comparison was made between the input energy of fuel, fuel input exergy, shaft energy, exhaust gas exergy, energy transmission rate to water, rate of entropy generation, rate of exergy destruction, and performance efficiency of the blend in relation to diesel.

The requirement of input fuel energy is minimum at FIP of 260 bar for NBD-TNP nanofuel at 100 % EL. The increased FIP of 220, 240, 260, and 280 bar of NBD-TNP nanofuel shows less energy requirement compared to other test cases. Also, the available energy of shaft or exergy is maximum for the FIP of 260 bar for NBD-TNP nanofuel at 100 % EL. Further, the entropy generation is found to be a minimum for FIP of 260 bar for NBD-TNP nanofuel at 100 % EL. Furthermore, the maximum exergetic efficiency is 40.11 % for FIP of 260 bar for NBD-TNP nano fuel at 100 % EL. Fig. 4(a–f) shows the variation of energy, exergy, entropy generation and the exergetic efficiency for diesel and NBE-TNP nano fuel under different FIPs at 100 % EL.

3.2. Performance study

The BTE of the NBD-TNP nanofuel is minimum at a standard 200 bar FIP. The increment of FIP values increases the BTE for NBD-TNP nanofuel. The average increase of BTE for 220, 240, 260, and 280 bar are 2.07, 6.41, 8.41, and 6.75 %, respectively, when compared to diesel at a standard 200 bar FIP. The maximum BTE of 29.22 % is reported for NBD-TNP nanofuel at FIP of 260 bar and 100 % EL. Fig. 5 (a) reveals the trends of BTE with the EL for different FIP values. The increase in BTE with the increase of FIP up to 260 bar might be due to the face that an increase in FIP leads to shorter combustion duration and better fuel atomization, as reported in various studies. However, the specific effects of FIP on combustion depend on engine speed and EL [91]. The combustion process can
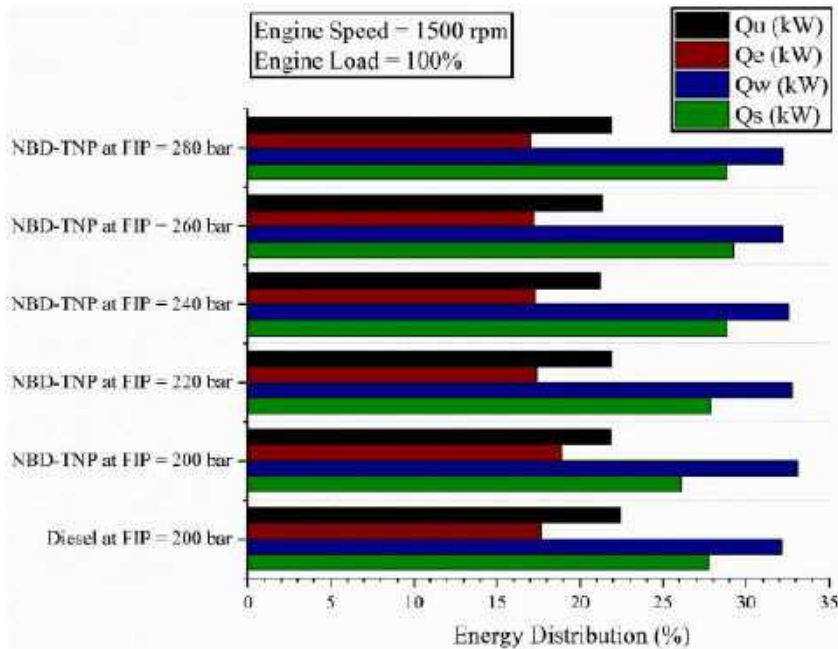

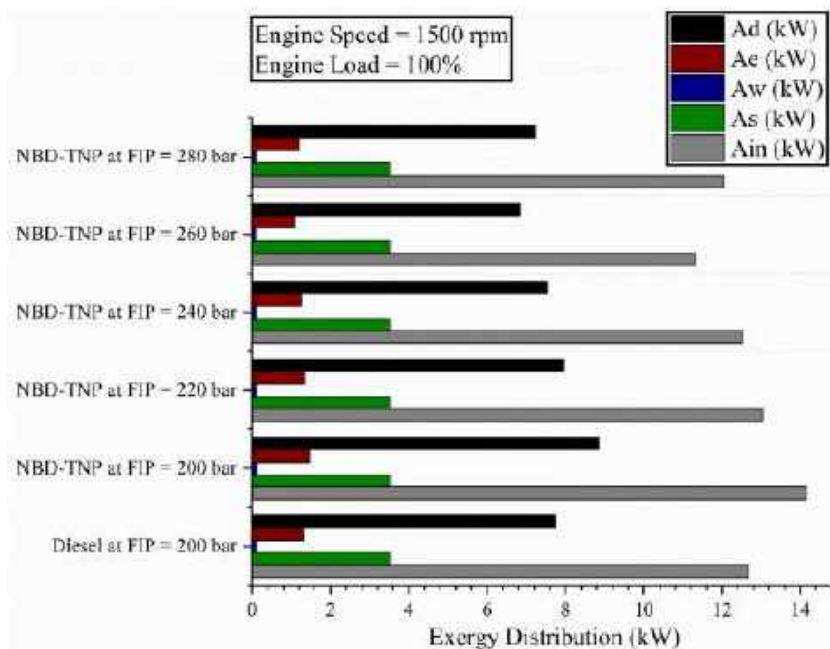**Fig. 4(b).** Energy Distribution (%) for different FIPs at 100 % EL.

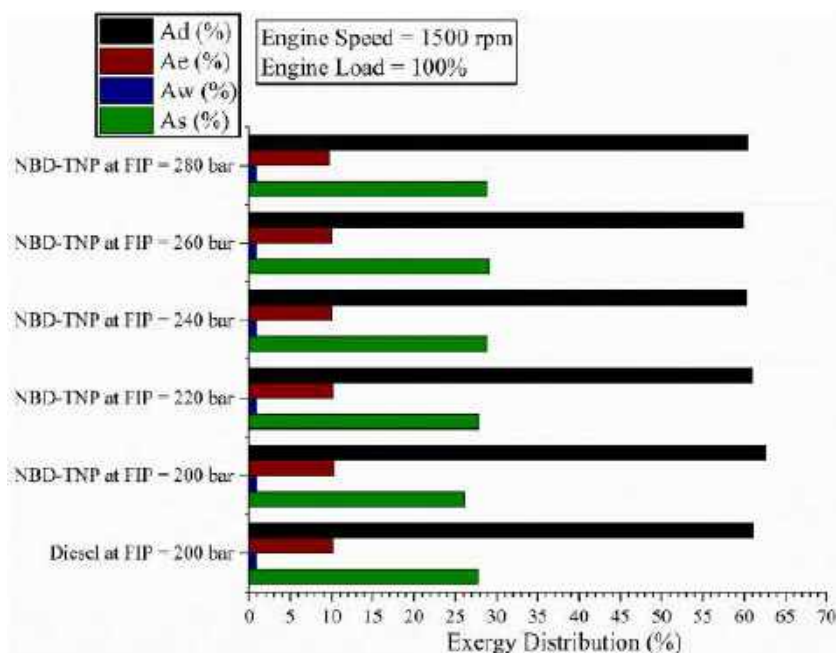**Fig. 4(c).** Exergy Distribution (kW) for different FIPs at 100 % EL.

Fig. 4(d). Exergy Distribution (%) for different FIPs at 100 % EL.

be improved by the enhanced atomization characteristics resulting from an increase in fuel injection pressure (FIP) [92]. Increment of the FIP value reduced the duration of ID, the amount of smoke emitted, the cylinder pressure, maximum rate of pressure rise, exhaust gas temperature, CO_2 emissions, while increased NOx emission [93]. An increase in FIP leads to improved BTE and combustion characteristics. The emission of CO, HC, and smoke from diesel engines decreases with higher injection pressure. Faster fuel evaporation, better fuel air mixture, and higher fuel atomization are the outcomes of increased FIP [94]. Due to the rise in FIP, the flame takes on a conical shape, becoming wider but shorter in length. As a result, the flame's penetration length decreases, and a larger flame reaction zone form, resulting in a voluminous flame. Additionally, increasing the FIP reduces the size of fuel droplets and improves
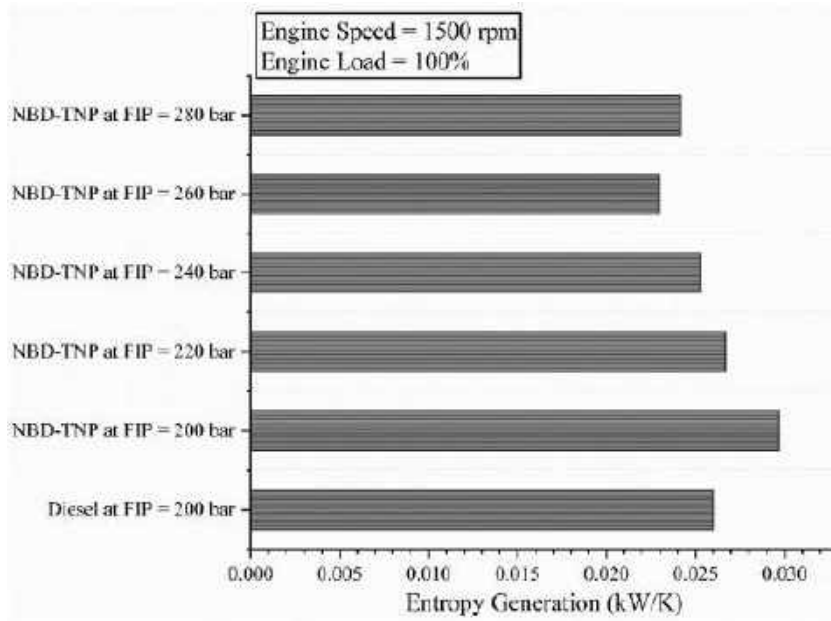
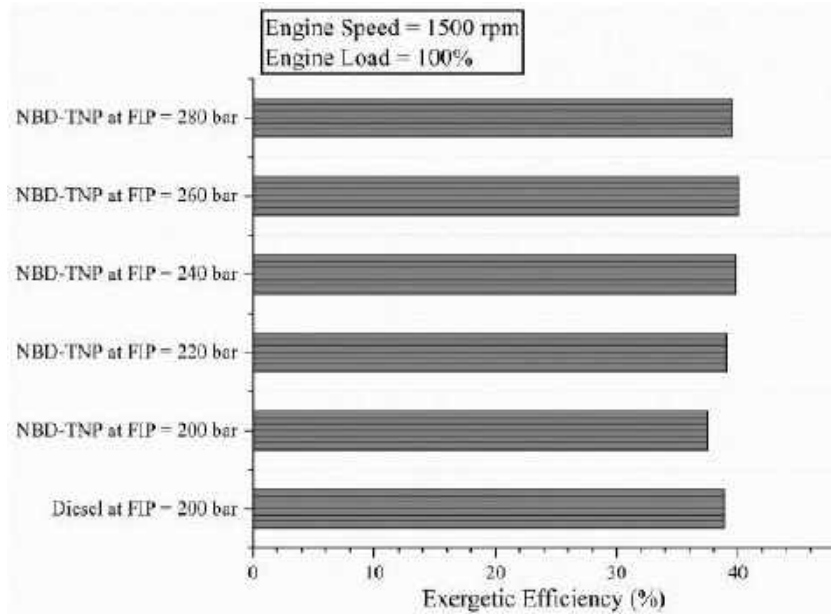**Fig. 4(e).** Entropy Generation (kW/K) for different FIPs at 100 % EL.

Fig. 4(f). Exergetic Efficiency for different FIPs at 100 % EL.

mixing, leading to higher temperatures and increased total radiation of the flame, while also reducing CO emissions and soot particles [95]. The increment of FIP reduces the duration of combustion [96]. High FIPs provides higher dispersion of fuel particles along with improved atomization and formation of air-fuel mixture. Additionally, there is enhanced evaporation of fine fuel particles which shortens ID. There is less chances of fuel adhering on the walls of the combustion chamber and produces less amount of emissions. Also, smoke and PM emissions reduces with high FIPs [97]. Further increase of FIPs beyond a certain limit lowers the performance, may be due to 'wet wall' problems which leads to incomplete combustion, when the FIP is too high, the "wet wall" effect will also affect the fuel–air mixing process, which is not conducive to ignition and combustion inside the cylinder, ultimately causing a decrease in the performance [98]. Moreover, excessively high FIP leads to combustion deterioration [96].

The minimum value of exhaust gas temperature (EGT) is found to be 302 °C for the NBD-TNP nanofuel at FIP of 260 bar and 100 % EL. The average decrease of EGT for 240, 260, and 280 bar are 0.33, 5.98, and 2.57 %, respectively, compared to diesel at a standard
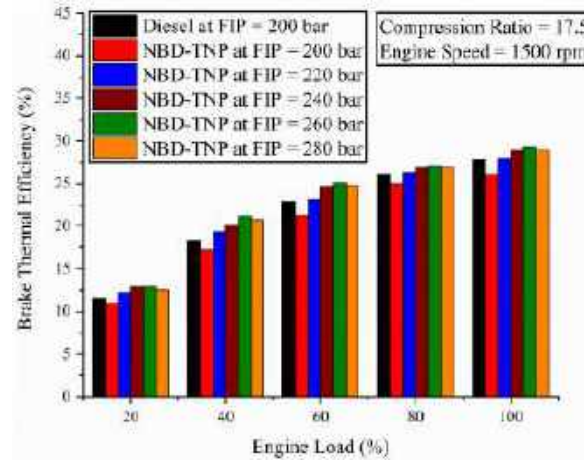
Fig. 5(a). BTE variation with EL and FIP.

FIP of 200 bar. The mean increase of EGT for 200 and 220 bar is 4.82 and 3.32 %, respectively, compared to diesel at a standard 200 bar FIP. Fig. 5 (b) portrays the changes of EGT with the EL for different FIP values.

The maximum value of peak cylinder pressure (PCP) is reported to be 336.93 bar for the NBD-TNP nanofuel at FIP of 260 bar and 100 % EL. The average increase of PCP for 220, 240, 260 and 280 bar are 3.1, 6.1, 9.63 and 7.64 %, respectively, compared to diesel at a standard FIP of 200 bar. The average decrease of PCP for 200 bar is 2.48 % compared to diesel at a standard 200 bar FIP. Fig. 5 (c) reveals the variation of PCP with the EL for different FIP values.

The maximum value of net heat release rate (NHRR) is reported to be 67.86 J/°CA for the NBD-TNP nanofuel at FIP of 260 bar and 100 % EL. The average increase of PCP for 220, 240, 260 and 280 bar are 0.32, 2.1, 9.54 and 4.66 %, respectively, compared to diesel at a standard 200 bar FIP. The mean decrease of NHRR for 200 bar is 1.66 % compared to diesel at a standard 200 bar FIP. Fig. 5 (d) displays the trends of NHRR with the EL for different FIP values.

The smallest ID is found for the NBD-TNP nanofuel at 260 bar FIP. The mean reduction of ID for 200, 220, 240, 260 and 280 bar are 12.9 %, 18.28 %, 21.5 %, 30.1 % and 24.73 %, correspondingly, compared to diesel at standard FIP of 200 bar. Fig. 5 (e) portrays the ID variation with the EL for different FIP values.

3.3. Emission study

The lowest CO emission for the NBD-TNP nanofuel at an FIP of 260 bar and 100 % EL is 42 ppm. The average decrease in CO emissions for 200, 220, 240, 260, and 280 bar are 24.2 %, 33.65 %, 40.88 %, 47.8 %, and 34.9 %, respectively, compared with diesel at standard 200 bar FIP. Fig. 6 (a) portrays the variation of CO emissions with the EL for different FIP values.

The minimum HC emission is 42 ppm for the NBD-TNP nanofuel at FIP of 260 bar and 100 % EL. The average reduction in HC emissions for 220, 240, and 260 bar are 3.55 %, 3.77 % and 4.22 %, respectively, as compared with diesel at a standard 200 bar FIP.
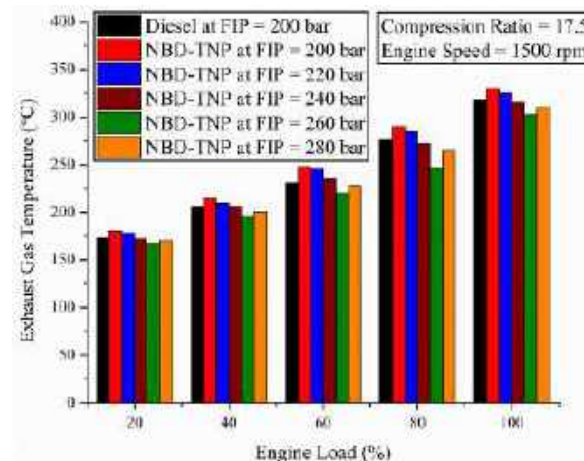

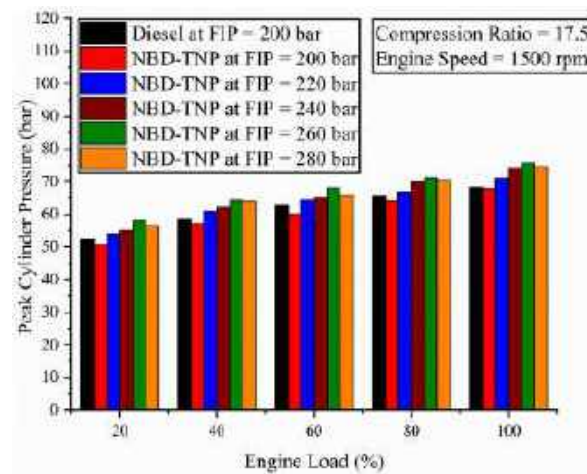**Fig. 5(b).** EGT variation with EL and FIP.
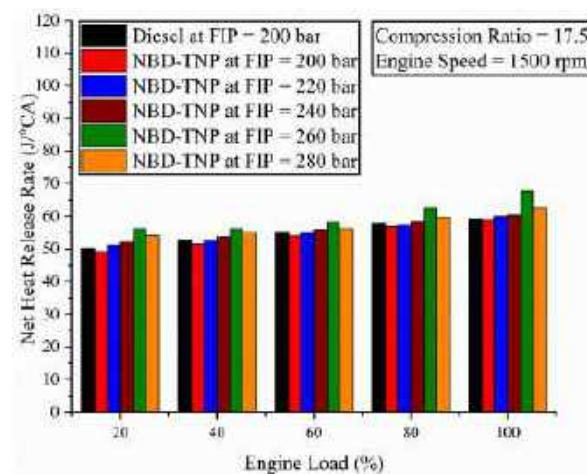
Fig. 5(c). PCP variation with EL and FIP.
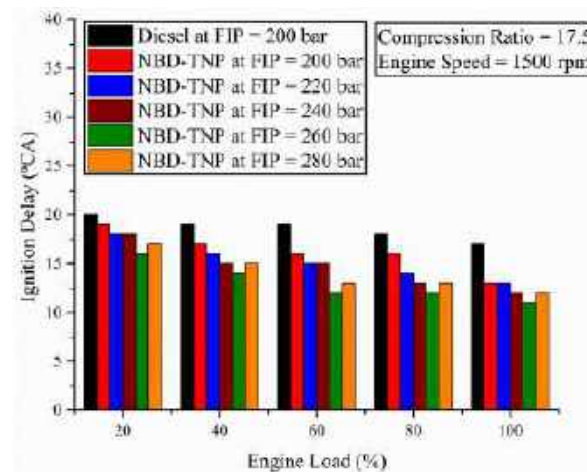

Fig. 5(d). NHRR variation with EL and FIP.

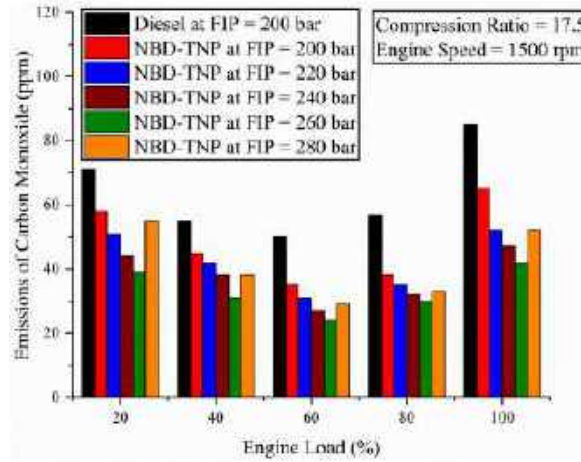**Fig. 5(e).** ID variation with EL and FIP.

Fig. 6(a). Emission of CO variation with EL and FIP.

Fig. 6 (b) portrays the variation of HC emissions with the EL for different FIP values. The average increase of HC emissions for 200 and 280 bar are 8.22 % and 6.22 %, respectively, as compared with diesel at a standard 200 bar FIP.

The average CO_2 emissions are minimum for the NBD-TNP nanofuel at 200 bar FIP. The average decrease in CO_2 emissions for 260 and 280 bar are 6.63 % and 2.35 %, respectively, compared to diesel at a standard 200 bar FIP. Fig. 6 (c) portrays the change of CO_2 emissions with the EL for different FIP values. The average increase of CO_2 emission for 200, 220, and 240 bar are 15.33 %, 11.33 % and 6.08 %, respectively, as compared with diesel at a standard 200 bar FIP.

The maximum NOx emission is 198 ppm for the NBD-TNP nanofuel at FIP of 260 bar and 100 % EL. The average increase in NOx emissions for 220, 240, 260 and 280 bar are 5.23 %, 8.53 %, 17.17 % and 11.05 %, respectively, as compared with diesel at a standard 200 bar FIP. Fig. 6 (d) reveals the variations in the values of NOx emissions with the EL for different FIP values. The mean decrease of NOx emission for 200 bar is 6.23 %, respectively, as compared with diesel at standard 200 bar FIP.

3.4. Statistical optimization

This study employs Response Surface Methodology (RSM) with a second-order quadratic polynomial model. This model captures the input variables' linear, quadratic, and interaction effects: engine load (EL) and fuel injection pressure (FIP). The model's goodness of fit was validated through three key statistical metrics: R^2 (Coefficient of Determination), which represents the proportion of variance explained by the model; Adjusted R^2, which accounts for the number of predictors to ensure a fair comparison; and Predicted R^2, which indicates how well the model predicts new data points [52]. The values shown in Table 4 illustrate a high degree of fit, confirming the reliability of the developed models. Additionally, p-values were used to evaluate the statistical significance of each coefficient, with values below 0.05 indicating significant contributions to the model [53].

The optimization was performed using the desirability function method in Design Expert software. The aim was to enhance BTE
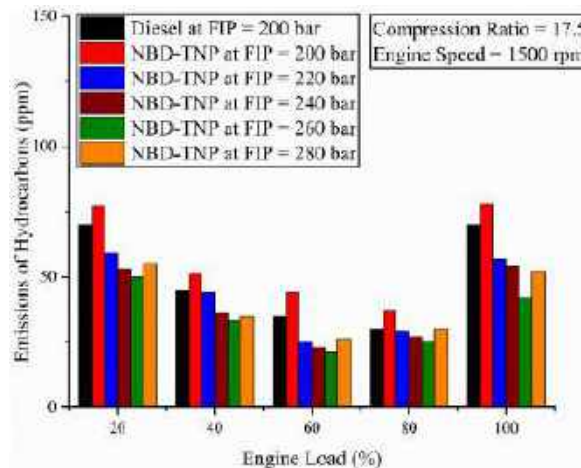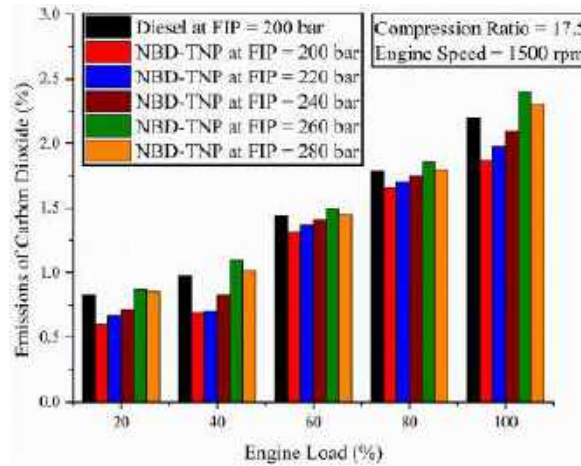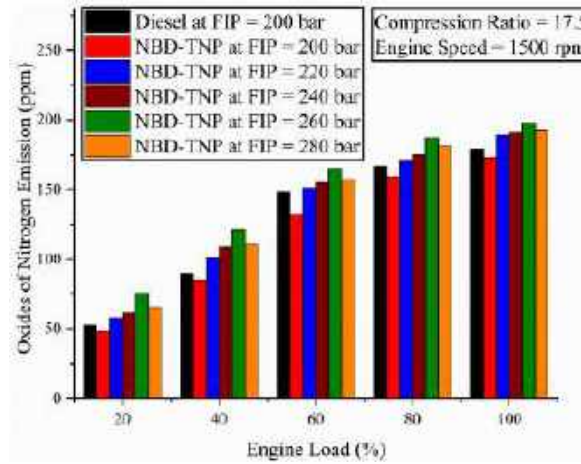

Fig. 6(b). Emission of HC variation with EL and FIP.

Fig. 6(c). Emission of CO_2 variation with EL and FIP.

Fig. 6(d). Emission of NOx variation with EL and FIP.

while reducing emissions (CO, HC, NOx) and keeping other performance metrics within acceptable ranges. The desirability function provides a score from 0 to 1 for each response, with 1 indicating the most favorable outcome. The overall desirability score is computed as the geometric mean of the individual desirability values. The best combination of input variables (EL and FIP) that maximized the overall desirability score is shown in Table 6, alongside the expected response values for each parameter.

To display the influences of EL and FIP on every response variable, 3D surface plots were created using Design Expert software (Fig. 7a–i). These plots reveal the connections between input variables and responses, showcasing both linear and nonlinear effects. Furthermore, the desirability plot (Fig. 7j) illustrates the combined optimization findings, where the peak signifies the optimal settings that enhance overall performance while minimizing emissions.

RSM is performed by considering the engine load and FIP as input variables and BTE, EGT, PSP, NHRR, ID, CO, HC, CO_2, and NOx as response variables. Table 3 shows the design matrix obtained from the experimental results that are used for RSM optimization. Table 4 reveals the goodness of fit of the generated model. Table 5 discloses the coefficient matrix, and equations 19–27 show the relationship between input and response variables. Fig. 7(a–i) shows the 3-D surface plots obtained from Design Expert software. Fig. 7 (j) reveals the desirability values of different parameters. Table 6 reveals the solution for optimized input and optimum value response parameters.

$$BTE = -48.22 + 0.4544\, EL + 0.4117\, FIP - 0.002284\, EL^2 - 0.000795\, FIP^2 + 0.000051\, EL*FIP \qquad \text{Eqn. 19}$$

$$EGT = 371 + 1.734\, EL - 1.735\, FIP + 0.00579\, EL^2 + 0.00336\, FIP^2 - 0.00278\, EL*FIP \qquad \text{Eqn. 20}$$

$$PCP = -59.1 + 0.2666\, EL + 0.843\, FIP - 0.000801\, EL^2 - 0.001607\, FIP^2 + 0.000169\, EL*FIP \qquad \text{Eqn. 21}$$
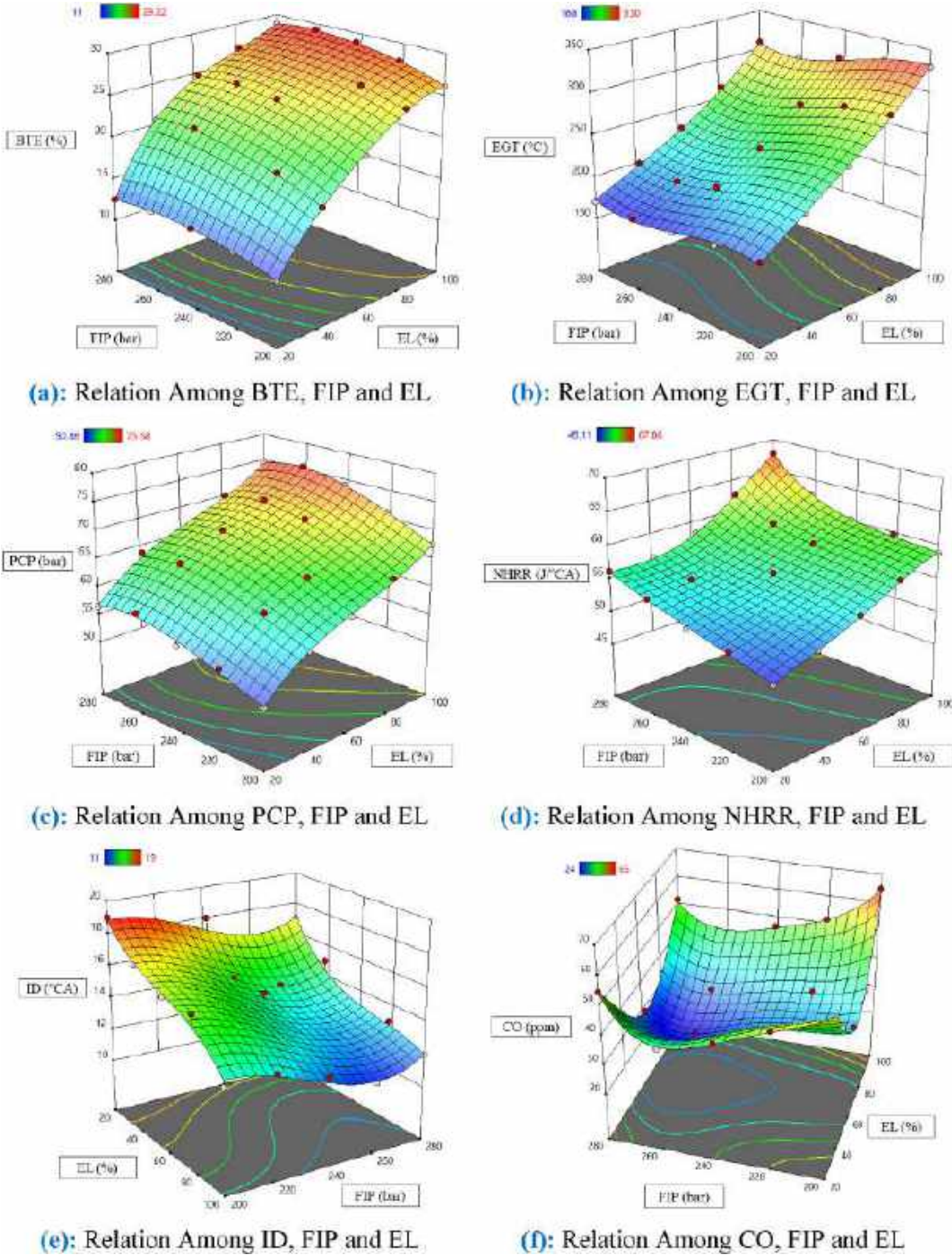
Fig. 7. Plots obtained from RSM optimization. **(a)**: Relation among BTE, FIP and EL. **(b)**: Relation among EGT, FIP and EL. **(c)**: Relation among PCP, FIP and EL. **(d)**: Relation among NHRR, FIP and EL. **(e)**: Relation among ID, FIP and EL. **(f)**: Relation among CO, FIP and EL. **(g)**: Relation among HC, FIP and EL. **(h)**: Relation among CO_2, FIP and EL. **(i)**: Relation among NOx, FIP and EL. (j): Desirability plot

$$NHRR = 73.7 - 0.0257\ EL - 0.249\ FIP + 0.000792\ EL^2 + 0.000645\ FIP^2 + 0.000213\ EL*FIP \qquad \text{Eqn. 22}$$

$$ID = 58.5 - 0.1221\ EL - 0.293\ FIP + 0.000393\ EL^2 + 0.000536\ FIP^2 + 0.000050\ EL*FIP \qquad \text{Eqn. 23}$$

(g): Relation Among HC, FIP and EL

(h): Relation Among CO_2, FIP and EL

(i): Relation Among NOx, FIP and EL
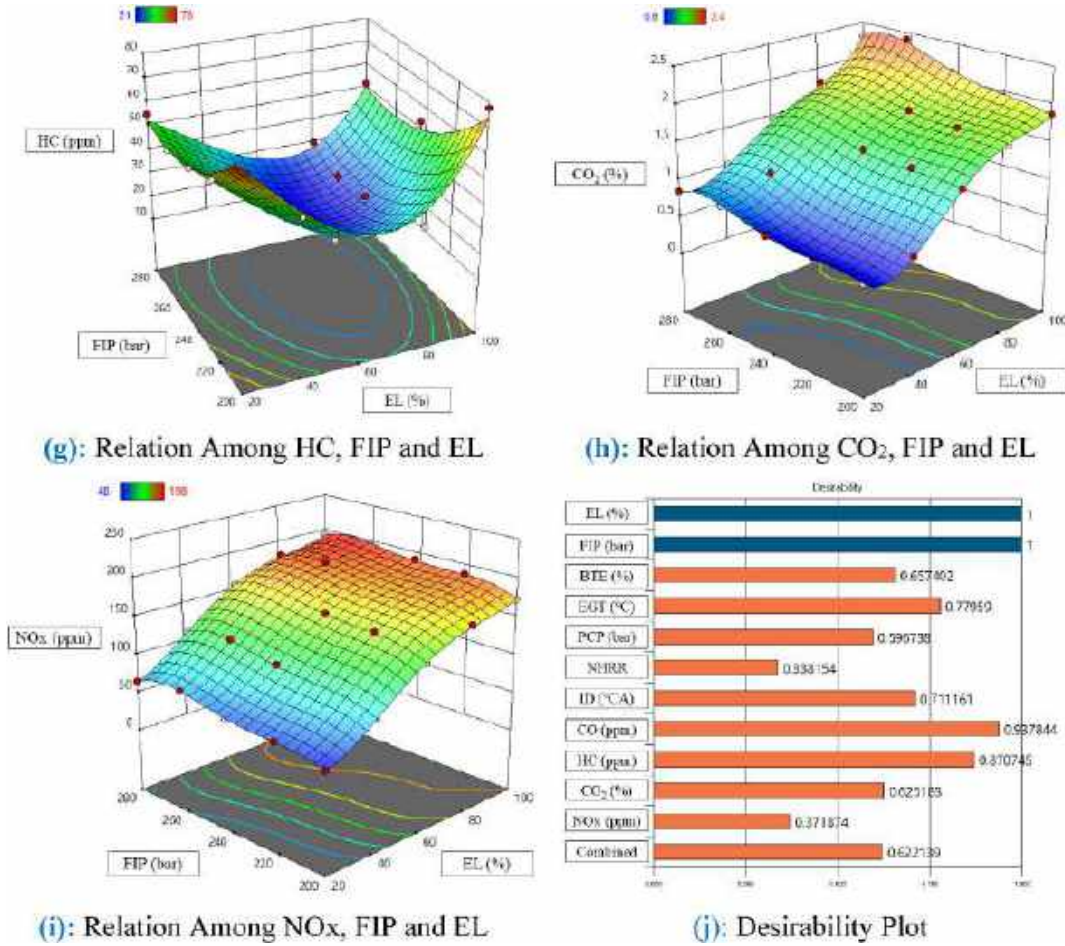

(j): Desirability Plot

Fig. 7. (*continued*).

$$CO = 384.2 - 1.374 \, EL - 2.525 \, FIP + 0.01271 \, EL^2 + 0.00511 \, FIP^2 - 0.000650 \, EL*FIP \qquad \text{Eqn. 24}$$

$$HC = 555.4 - 2.322 \, EL - 3.628 \, FIP + 0.01889 \, EL^2 + 0.00711 \, FIP^2 - 0.00007 \, EL*FIP \qquad \text{Eqn. 25}$$

$$CO_2 = -1.63 + 0.00847 \, EL + 0.0143 \, FIP + 0.000055 \, EL^2 - 0.000024 \, FIP^2 + 0.000014 \, EL*FIP \qquad \text{Eqn. 26}$$

$$NOx = -464.8 + 3.507 \, EL + 3.577 \, FIP - 0.01493 \, EL^2 - 0.00679 \, FIP^2 - 0.00040 \, EL*FIP \qquad \text{Eqn. 27}$$

3.5. Implications of the study

The study's implications are extensive and profoundly impact emissions reduction, engine performance, and the development of sustainable fuels. First off, the findings of this study on the combination of Nahar Biodiesel and TiO_2 nanoparticles have essential ramifications for improving engine performance indicators such as power output, combustion efficiency, and BTE. This might open the door for creating dependable and more efficient diesel engines, advancing the power generating and automobile sectors. Second, the study's emphasis on lowering emissions and improving fuel injection settings is consistent with international environmental objectives. The study aids in tackling air pollution and climate change issues by reducing hazardous pollutants such as NOx, HC, and CO. In addition, the advancement of sustainable projects, the decrease in reliance on fossil fuels, and the acceleration of the shift to a low-carbon economy are all facilitated by the promotion of renewable energy sources like Nahar Biodiesel. These ramifications affect how policies are formulated, how technology is developed, and how businesses operate in the transportation and energy sectors.

4. Conclusions

The present study investigates the thermodynamic performance, emissions characteristics, and statistical optimization of a single-cylinder diesel engine using NBD-TNP nanofuel at varying FIPs and ELs. Based on the obtained data, the following regular rules and

Table 3
Design matrix.

EL	FIP	BTE	EGT	PCP	NHRR	ID	CO	HC	CO$_2$	NOx
20	200	11	180	50.88	49.11	19	58	77	0.6	48
40	200	17.22	214	57.11	51.34	17	45	51	0.69	85
60	200	21.33	248	60.11	53.99	16	35	44	1.31	132
80	200	25	290	63.99	56.99	16	38	37	1.66	159
100	200	26.11	330	67.62	58.93	13	65	78	1.87	173
20	220	12.19	178	54.11	51.11	18	51	59	0.67	58
40	220	19.32	210	60.77	52.66	16	42	44	0.7	101
60	220	23.11	246	64.22	54.88	15	31	25	1.37	151
80	220	26.3	285	66.67	57.22	14	35	29	1.7	171
100	220	27.87	325	71.11	59.96	13	52	57	1.98	189
20	240	12.87	172	55	52.11	18	44	53	0.71	61
40	240	20.11	206	62.11	53.77	15	38	36	0.83	109
60	240	24.66	235	65.11	55.99	15	27	23	1.41	155
80	240	26.9	272	69.89	58.5	13	32	27	1.75	175
100	240	28.87	315	74	60.35	12	47	54	2.1	191
20	260	12.91	168	57.89	54.11	16	39	50	0.87	75
40	260	21.2	195	64.22	54.99	14	31	33	1.1	121
60	260	25.1	220	67.91	56.21	12	24	21	1.5	165
80	260	27.11	247	71.33	59.77	12	30	25	1.85	187
100	260	29.22	302	75.58	62.67	11	42	42	2.4	198
20	280	12.5	170	56.44	56.22	17	55	55	0.85	65
40	280	20.71	200	63.77	56.22	15	38	35	1.01	111
60	280	24.8	228	66	58.21	13	29	26	1.45	157
80	280	26.9	265	70.11	62.67	13	33	30	1.8	181
100	280	28.87	310	74.49	67.86	12	52	52	2.3	193

Table 4
Goodness of fit.

Variable	R^2 (%)	R^2 (adj.) (%)	R^2 (pred.) (%)
BTE	99.31	99.13	98.81
EGT	98.94	98.66	98.22
PCP	98.42	98.01	97.45
NHRR	96.59	95.69	91.59
ID	91.5	89.27	84
CO	88.97	86.07	78.98
HC	92.87	91	85.83
CO$_2$	96.66	95.79	94.42
NOx	99.23	99.03	98.67

Table 5
Coefficient matrix.

	Intercept	EL	FIP	EL*IP	EL^2	FIP^2
BTE	24.4236	6.34119	1.65267	−1.30067	−2.72722	−0.972884
p-values		<0.0001	<0.0001	0.0067	0.0021	0.1723
EGT	233.126	63.8667	−29.1	−4.44	9.25714	5.37143
p-values		<0.0001	<0.0001	0.0117	0.0002	0.0109
PCP	66.3439	6.35857	4.264	0.27	−1.28171	−2.57086
p-values		<0.0001	<0.0001	0.3211	0.0010	<0.0001
NHRR	55.6729	4.73805	1.29305	−0.211133	1.89527	0.191605
p-values		<0.0001	0.0011	0.6894	0.0587	0.8336
ID	13.8571	−1.55714	−2.90952	0.08	0.628571	0.857143
p-values		0.0086	<0.0001	0.7275	0.0339	0.0062
CO	28.729	−7.07143	−10.0095	7.57333	25.3354	−6.76463
p-values		0.0001	<0.0001	0.0045	<0.0001	0.0890
HC	21.72	−13.5476	−5.67143	−0.12	30.2286	11.3714
p-values		0.0010	0.1074	0.9351	<0.0001	<0.0001
CO$_2$	1.38737	0.961952	0.256286	−0.159333	−0.534143	0.292857
p-values		<0.0001	<0.0001	0.0397	0.0010	0.0309
NOx	154.576	70.919	18.3143	−7.89333	−56.666	19.1007
p-values		<0.0001	<0.0001	0.0221	<0.0001	0.0036

Table 6
Optimized parameters.

Parameter	Value
EL	47.948
FIP	263.455
BTE	22.977
EGT	203.697
PCP	65.618
NHRR	55.45
ID	13.311
CO	26.551
HC	28.373
CO_2	1.275
NOx	142.204
Desirability	0.622

conclusions are summarized:

- Optimal Fuel Injection Pressure (FIP): Increasing FIP improves engine performance and reduces emissions up to an optimal level of 260 bar, beyond which performance deteriorates due to incomplete combustion caused by the "wet wall" effect.
- Engine Load (EL) Influence: Higher engine loads (80–100 %) lead to improved BTE, NHRR, and PCP due to better fuel-air mixing and combustion, while lower loads increase emissions due to incomplete combustion.
- Energy and Exergy Optimization: Maximum exergetic efficiency (40.11 %) and BTE (29.22 %) are achieved at 260 bar FIP and 100 % EL, highlighting the importance of balancing energy utilization and reducing entropy generation.
- Emission Reduction Trends: CO and HC emissions decrease as FIP increases due to enhanced atomization and combustion efficiency, with the lowest emissions recorded at 260 bar. However, NOx emissions increase with higher FIP due to elevated combustion temperatures.
- Nanoparticle Effect: TiO_2 nanoparticles improve fuel combustion by shortening ignition delay, increasing BTE, and reducing CO and HC emissions due to catalytic oxidation of carbon particles.
- Statistical Optimization: Using RSM, the optimal combination of 47.95 % EL and 263.45 bar FIP yields balanced performance and emissions, with a desirability score of 0.622. This demonstrates that partial engine load can achieve near-optimal results while conserving fuel.

These findings suggest optimizing FIP and EL within the identified ranges improves engine efficiency, reduces emissions, and sustains fuel utilization. The results validate NBD-TNP nano fuel as a viable alternative to diesel fuel, especially at an FIP of 260 bar, supporting the transition to greener energy solutions.

4.1. Limitations

There are a few constraints to consider, even if the study provides insightful information about combining TiO_2 nanoparticles with Nahar Biodiesel in diesel engines. First, the study's experimental scope could be restricted to particular engine combinations, fuel mixes, and operating parameters, which might limit how broadly the results can be applied to various diesel engines and real-world driving situations. Second, further research is needed to determine how nanoparticles interact with engine parts and biodiesel, as well as any possible effects on the environment and practicality from an economic standpoint. Furthermore, the research may not fully cover certain areas of regulatory compliance pertaining to safety procedures, emissions limits, and fuel quality requirements. Acknowledging and resolving these constraints via more investigation and evaluation will lead to a more thorough comprehension of the difficulties and prospects of using mixes of biodiesel and nanoparticles in diesel engines.

4.2. Future scope

The NBD-TNP nanofuel used in this study has been focused on FIP variation. Further, other operating parameters, such as injection timing, compression ratio, and exhaust gas recirculation, along with the variation of the type of nanoparticles, may be varied to achieve maximum exergy and BTE output as well as to reduce emissions.

CRediT authorship contribution statement

Akshay Jain: Data curation, Conceptualization. **Bhaskor Jyoti Bora:** Investigation, Formal analysis. **Rakesh Kumar:** Methodology, Investigation, Data curation. **Debabrata Barik:** Resources, Project administration, Methodology. **Nithin Kumar:** Supervision, Software, Resources. **Prabhu Paramasivam:** Visualization, Validation. **Raman Kumar:** Writing – review & editing, Visualization, Supervision. **Jasgurpreet Singh Chohan:** Supervision, Software. **Hasan Sh Majdi:** Visualization, Funding acquisition. **Majed Alsubih:** Supervision, Resources, Funding acquisition. **Saiful Islam:** Validation, Funding acquisition, Formal analysis. **Chander**

Prakash: Writing – review & editing, Visualization, Supervision. **Rahul Kumar:** Writing – review & editing, Visualization, Software.

Declaration of competing interest

The authors declare that they have no known competing financial interests or personal relationships that could have appeared to influence the work reported in this paper.

Acknowledgement

Data availability

The data that support the findings are included within the manuscript itself.

References

[1] P.M. Rao, S.H. Dhoria, S.G.K. Patro, R.K. Gopidesi, M.Q. Alkahtani, S. Islam, M. Vijaya, J.L. Jayanthi, M.A. Khan, A. Razak, et al., Artificial intelligence based modelling and hybrid optimization of linseed oil biodiesel with graphene nanoparticles to stringent biomedical safety and environmental standards, Case Stud. Therm. Eng. 51 (2023), https://doi.org/10.1016/j.csite.2023.103554.

[2] M. Kumar, H.S. Farwaha, R. Kumar, T.Y. Khan, S. Javed, A.K. Sachdeva, S. Singh, A. Rizal, M.I. Ammarullah, Thermal performance evaluation of solar collector with rice husk Graphene-PCM: bioengineering approach, Case Stud. Therm. Eng. (2023) 103773.

[3] M. Arun, D. Barik, S. Chandran, N. Govil, P. Sharma, T.M. Yunus Khan, R.U. Baig, B.J. Bora, B.J. Medhi, R. Kumar, et al., Twisted helical Tape's impact on heat transfer and friction in zinc oxide (ZnO) nanofluids for solar water heaters: biomedical insight, Case Stud. Therm. Eng. (2024) 104204, https://doi.org/10.1016/j.csite.2024.104204.

[4] E.R. Babu, N.C. Reddy, A. Babbar, A. Chandrashekar, R. Kumar, P.S. Bains, M. Alsubih, S. Islam, S.K. Joshi, A. Rizal, et al., Characteristics of pulsating heat pipe with variation of tube diameter, filling ratio, and SiO2 nanoparticles: biomedical and engineering implications, Case Stud. Therm. Eng. 55 (2024) 104065, https://doi.org/10.1016/j.csite.2024.104065.

[5] P. Das, C.K. Jha, S. Saxena, R.K. Ghosh, Can biofuels help achieve sustainable development goals in India? A systematic review, Renew. Sustain. Energy Rev. 192 (2024) 114246, https://doi.org/10.1016/j.rser.2023.114246.

[6] K.-W. Jeon, J.-H. Gong, M.-J. Kim, J.-O. Shim, W.-J. Jang, H.-S. Roh, Review on the production of renewable biofuel: solvent-free deoxygenation, Renew. Sustain. Energy Rev. 195 (2024) 114325, https://doi.org/10.1016/j.rser.2024.114325.

[7] Z. Yang, K. Shah, C. Pilon-McCullough, R. Faragher, P. Azmi, B. Hollebone, B. Fieldhouse, C. Yang, D. Dey, P. Lambert, et al., Characterization of renewable diesel, petroleum diesel and renewable diesel/biodiesel/petroleum diesel blends, Renew. Energy 224 (2024) 120151, https://doi.org/10.1016/j.renene.2024.120151.

[8] P. Kalita, B. Basumatary, P. Saikia, B. Das, S. Basumatary, Biodiesel as renewable biofuel produced via enzyme-based catalyzed transesterification, Energy Nexus 6 (2022) 100087, https://doi.org/10.1016/j.nexus.2022.100087.

[9] R.K. Mohan, J. Sarojini, Ü. Ağbulut, U. Rajak, T.N. Verma, K.T. Reddy, Energy recovery from waste plastic oils as an alternative fuel source and comparative assessment of engine characteristics at varying fuel injection timings, Energy 275 (2023) 127374, https://doi.org/10.1016/j.energy.2023.127374.

[10] U. Rajak, V. Nageswara Reddy, Ü. Ağbulut, S. Sarıdemir, A. Afzal, T. Nath Verma, Modifying diesel fuel with nanoparticles of zinc oxide to investigate its influences on engine behaviors, Fuel 345 (2023) 128196, https://doi.org/10.1016/j.fuel.2023.128196.

[11] T. Subhaschandra Singh, T. Nath Verma, P. Nashine, Analysis of an anaerobic digester using numerical and experimental method for biogas production, Mater. Today Proc. 5 (2018) 5202–5207, https://doi.org/10.1016/j.matpr.2017.12.102.

[12] C.Tiwari; T.N.Verma; G.Dwivedi, Optimization of biodiesel production parameters for hybrid oil using RSM and ANN technique and its effect on engine performance, combustion, and emission characteristics. Proc. Inst. Mech. Eng. Part E J. Process Mech. Eng. 0, 09544089241241130, doi:10.1177/09544089241241130..

[13] H. Guo, Y. Li, B. Zhao, Y. Guo, Z. Xie, A. Morina, X. Lu, Transient lubrication of floating bush coupled with dynamics and kinematics of cam-roller in fuel supply mechanism of diesel engine, Phys. Fluids 36 (2024) 123103, https://doi.org/10.1063/5.0232226.

[14] J. Shi, B. Zhao, X. Niu, Q. Xin, H. Xu, X. Lu, Time-varying dynamic characteristic analysis of journal–thrust coupled bearings based on the transient lubrication considering thermal-pressure coupled effect, Phys. Fluids 36 (2024) 083116, https://doi.org/10.1063/5.0217495.

[15] A. Haghparast, J. Zarringhalam, A. Khatibi, E. Dianati, J. Shams, The fruit essential oil of Cuminum cyminum L. reduced the acquisition but not expression of ineffective dose of morphine-induced conditioned place preference in morphine- sensitized mice, J. Med. Plant 8 (2009) 64–74.

[16] A. Jain, B. Jyoti Bora, P. Sharma, R. Kumar, B. Jyoti Medhi, D. Balakrishnan, N. Senthilkumar, Statistical analysis of Mesua Ferrea seed oil biodiesel fueled diesel engine at variable injection timings using response surface methodology, Sustain. Energy Technol. Assessments 60 (2023) 103476, https://doi.org/10.1016/j.seta.2023.103476.

[17] S.H. Dhawane, S. Chowdhury, G. Halder, Lipase immobilised carbonaceous catalyst assisted enzymatic transesterification of Mesua ferrea oil, Energy Convers. Manag. 184 (2019) 671–680, https://doi.org/10.1016/j.enconman.2019.01.038.

[18] A.P. Bora, S.H. Dhawane, K. Anupam, G. Halder, Biodiesel synthesis from Mesua ferrea oil using waste shell derived carbon catalyst, Renew. Energy 121 (2018) 195–204, https://doi.org/10.1016/j.renene.2018.01.036.

[19] P. Bora, J. Boro, L.J. Konwar, D. Deka, A comparative study of Mesua ferrea L. based hybrid fuel with diesel fuel and biodiesel, Energy Sources, Part A Recovery, Util. Environ. Eff. 38 (2016) 1279–1285, https://doi.org/10.1080/15567036.2012.747036.

[20] N. Bordoloi, R. Narzari, R.S. Chutia, T. Bhaskar, R. Kataki, Pyrolysis of Mesua ferrea and Pongamia glabra seed cover: characterization of bio-oil and its sub-fractions, Bioresour. Technol. 178 (2015) 83–89, https://doi.org/10.1016/j.biortech.2014.10.079.

[21] Y.S. Kushwah, P. Mahanta, S.C. Mishra, Some studies on fuel characteristics of Mesua Ferrea, Heat Transf. Eng. 29 (2008) 405–409, https://doi.org/10.1080/01457630701825788.

[22] S.K. Dash, P. Lingfa, S.B. Chavan, An experimental investigation on the application potential of heterogeneous catalyzed Nahar biodiesel and its diesel blends as diesel engine fuels, Energy Sources, Part A Recovery, Util. Environ. Eff. 40 (2018) 2923–2932, https://doi.org/10.1080/15567036.2018.1514433.

[23] S.K. Dash, P. Lingfa, S.B. Chavan, Combustion analysis of a single cylinder variable compression ratio small size agricultural DI diesel engine run by Nahar biodiesel and its diesel blends, Energy Sources, Part A Recovery, Util. Environ. Eff. 42 (2020) 1681–1690, https://doi.org/10.1080/15567036.2019.1604878.

[24] M. Dabi, B.B. Sahoo, U.K. Saha, Increase of efficiency and reduction of CO and NOx emissions in a stationary compression ignition engine run on Mesua ferrea linn oil-diesel and diethyl ether, Therm. Sci. Eng. Prog. 25 (2021) 100980, https://doi.org/10.1016/j.tsep.2021.100980.

[25] M. Dabi, U. Saha, Influence of ethanol on the performance, combustion and emission characteristics of a stationary diesel engine run on diesel–mesua ferrea linn oil blend, Sadhana 45 (2020) 285, https://doi.org/10.1007/s12046-020-01518-8.

[26] M. Dabi, U.K. Saha, Performance, combustion and emissions analyses of a single-cylinder stationary compression ignition engine powered by Mesua Ferrea Linn oil-ethanol-diesel blend, Clean. Eng. Technol. 8 (2022) 100458, https://doi.org/10.1016/j.clet.2022.100458.

[27] L. Zhou, Q. Sun, S. Ding, S. Han, A. Wang, A machine-learning-based method for ship propulsion power prediction in ice, J. Mar. Sci. Eng. 11 (2023) 1381, https://doi.org/10.3390/jmse11071381.

[28] Q. Sun, J. Chen, L. Zhou, S. Ding, S. Han, A study on ice resistance prediction based on deep learning data generation method, Ocean Eng. 301 (2024) 117467, https://doi.org/10.1016/j.oceaneng.2024.117467.

[29] J. Hang, G. Qiu, M. Hao, S. Ding, Improved fault diagnosis method for permanent magnet synchronous machine system based on lightweight multisource information data layer fusion, IEEE Trans. Power Electron. 39 (2024) 13808–13817, https://doi.org/10.1109/TPEL.2024.3432163.

[30] Z. Xu, M. Wang, L. Chang, K. Pan, X. Shen, S. Zhong, L. Chen, Assessing the particulate matter emission reduction characteristics of small turbofan engine fueled with 100% HEFA sustainable aviation fuel, Sci. Total Environ. 945 (2024) 174128, https://doi.org/10.1016/j.scitotenv.2024.174128.

[31] X. Sun, Z. Li, L. Zhang, A. Tian, W.S. Chai, T. Jing, F. Qin, Heat transfer augmentation, endothermic pyrolysis and surface coking of hydrocarbon fuel in manifold microchannels at a supercritical pressure, Int. Commun. Heat Mass Tran. 161 (2025) 108564, https://doi.org/10.1016/j.icheatmasstransfer.2024.108564.

[32] H. Söyler, M.K. Balki, C. Sayin, The impact of injection timing and pressure on a CRDI engine's combustion characteristics, J. Eng. Res. (2024), https://doi.org/10.1016/j.jer.2024.02.015.

[33] C. Jit Sarma, P. Sharma, B.J. Bora, D.K. Bora, N. Senthilkumar, D. Balakrishnan, A.I. Ayesh, Improving the combustion and emission performance of a diesel engine powered with mahua biodiesel and TiO2 nanoparticles additive, Alex. Eng. J. 72 (2023) 387–398, https://doi.org/10.1016/j.aej.2023.03.070.

[34] H. Dave, D. Solanki, P. Naik, Effect of pilot fuel quantity and fuel injection pressure on combustion, performance and emission characteristics of an automotive diesel engine, Int. J. Thermofluids 21 (2024) 100570, https://doi.org/10.1016/j.ijft.2024.100570.

[35] S. Thiruvenkatachari, C.G. Saravanan, V. Raman, M. Vikneswaran, J.S.F. Josephin, E.G. Varuvel, An experimental study of the effects of fuel injection pressure on the characteristics of a diesel engine fueled by the third generation Azolla biodiesel, Chemosphere 308 (2022) 136049, https://doi.org/10.1016/j.chemosphere.2022.136049.

[36] C. Jin, J. Wei, B. Chen, X. Li, D. Ying, L. Gong, W. Fang, Effect of nanoparticles on diesel engines driven by biodiesel and its blends: a review of 10 years of research, Energy Convers. Manag. 291 (2023) 117276, https://doi.org/10.1016/j.enconman.2023.117276.

[37] M. El-Adawy, Effects of diesel-biodiesel fuel blends doped with zinc oxide nanoparticles on performance and combustion attributes of a diesel engine, Alex. Eng. J. 80 (2023) 269–281, https://doi.org/10.1016/j.aej.2023.08.060.

[38] M.S. Abishek, S. Kachhap, U. Rajak, T.N. Verma, T.S. Singh, S. Shaik, E. Cuce, M. Alwetaishi, Alumina and titanium nanoparticles to diesel–Guizotia abyssinica (L.) biodiesel blends on MFVCR engine performance and emissions, Sustain. Energy Technol. Assessments 61 (2024) 103580, https://doi.org/10.1016/j.seta.2023.103580.

[39] S. Kumar, R. Gautam, Energy and exergy assessment of diesel-tallow biodiesel blend in compression ignition engine for engine design variables, Sustain. Energy Technol. Assessments 57 (2023) 103305, https://doi.org/10.1016/j.seta.2023.103305.

[40] K. Bayramoğlu, M. Nuran, Energy, exergy, sustainability evaluation of the usage of pyrolytic oil and conventional fuels in diesel engines, Process Saf. Environ. Prot. 181 (2024) 324–333, https://doi.org/10.1016/j.psep.2023.11.034.

[41] A. Jain, B. Jyoti Bora, R. Kumar, C. Ahamed Saleel, P. Sharma, R. Ramaraj, D. Balakrishnan, Estimation of the potential of Nahar biodiesel run diesel engine at varying fuel injection pressures and engine loads through exergy approach, Alex. Eng. J. 84 (2023) 262–274, https://doi.org/10.1016/j.aej.2023.11.014.

[42] L. Chen, Y. Cao, X. Hu, B. Zhang, X. Chen, B. Cui, Z. Xu, Raman spectral optimization for soot particles: a comparative analysis of fitting models and machine learning enhanced characterization in combustion systems, Build. Environ. 271 (2025) 112600, https://doi.org/10.1016/j.buildenv.2025.112600.

[43] M.S. Gad, S. Jayaraj, A comparative study on the effect of nano-additives on the performance and emissions of a diesel engine run on Jatropha biodiesel, Fuel 267 (2020) 117168, https://doi.org/10.1016/j.fuel.2020.117168.

[44] B.J. Bora, U.K. Saha, Experimental evaluation of a rice bran biodiesel – biogas run dual fuel diesel engine at varying compression ratios, Renew. Energy 87 (2016) 782–790, https://doi.org/10.1016/j.renene.2015.11.002.

[45] H. Yu, H. Wang, Z. Lian, An assessment of seal ability of tubing threaded connections: a hybrid empirical-numerical method, J. Energy Resour. Technol. 145 (2022), https://doi.org/10.1115/1.4056332.

[46] Y. Dong, B. Xu, T. Liao, C. Yin, Z. Tan, Application of local-feature-based 3-D point cloud stitching method of low-overlap point cloud to aero-engine blade measurement, IEEE Trans. Instrum. Meas. 72 (2023), https://doi.org/10.1109/TIM.2023.3309384.

[47] S. Zhang, J. Li, Y. Tian, S. Fang, C. Li, X. Yu, L. Yang, Probing the combustion characteristics of micron-sized aluminum particles enhanced with graphene fluoride, Combust. Flame 272 (2025) 113858, https://doi.org/10.1016/j.combustflame.2024.113858.

[48] X. Zhang, Q. Zhu, S. Wang, T. Ma, S. Gao, Y. Kong, F. Chu, Hybrid triboelectric-variable reluctance generator assisted wireless intelligent condition monitoring of aero-engine main bearings, Nano Energy 136 (2025) 110721, https://doi.org/10.1016/j.nanoen.2025.110721.

[49] B.J. Bora, U.K. Saha, Comparative assessment of a biogas run dual fuel diesel engine with rice bran oil methyl ester, pongamia oil methyl ester and palm oil methyl ester as pilot fuels, Renew. Energy 81 (2015) 490–498, https://doi.org/10.1016/j.renene.2015.03.019.

[50] B.J. Bora, T. Dai Tran, K. Prasad Shadangi, P. Sharma, Z. Said, P. Kalita, A. Buradi, V. Nhanh Nguyen, H. Niyas, M. Tuan Pham, et al., Improving combustion and emission characteristics of a biogas/biodiesel-powered dual-fuel diesel engine through trade-off analysis of operation parameters using response surface methodology, Sustain. Energy Technol. Assessments 53 (2022) 102455, https://doi.org/10.1016/j.seta.2022.102455.

[51] S. Li, F. Wang, P. Rozga, X. Chen, Y. Zhang, B. Li, J. Li, The hidden vulnerabilities of pentaerythritol synthetic ester insulating oil for eco-friendly transformers: a dive into molecular behavior, IEEE Trans. Dielectr. Electr. Insul. (2024), https://doi.org/10.1109/TDEI.2024.3510476.

[52] X. Cao, J. Zhou, X. Zhou, Z. Wang, Z. Wang, Y. Sheng, Experimental research on the synergy effect of resistance/inhibition on the syngas explosion, Fuel 363 (2024) 130995, https://doi.org/10.1016/j.fuel.2024.130995.

[53] Z. Qiu, R. Chen, X. Gan, C. Wu, Torsional damper design for diesel engine: theory and application, Phys. Scri. 99 (2024) 125214, https://doi.org/10.1088/1402-4896/ad8af8.